CCDC11 Acts as a Scaffold to Assemble the ESCRT Membrane-Scission Machinery at Viral Budding Sites for HIV-1 Release: Identifying a Novel Therapeutic Strategy for Antiviral Therapy

Leo Takemaru

Ward Melville High School

Poojan Pandya

Half Hollow Hills High School West

Introduction

Coiled-Coil Domain-Containing 11 (CCDC11) was initially discovered as a gene mutated in human laterality disorder patients suffering from heterotaxy and *situs inversus* [1]. CCDC11 is a 514 aa protein that harbors three coiled-coil domains. Four unique human CCDC11 mutations have been reported to date [1-4]. Further studies showed that CCDC11 plays an important role in the establishment of left-right lateral asymmetry [2-5]. Interestingly, in animals, the left-right asymmetry of internal organs is determined during early embryogenesis through the function of cilia, small hair-like structures that are present on the surface of many cell types [6, 7]. Cilia are evolutionarily conserved microtubule-based organelles that protrude from the apical cell surface to perform diverse biological functions [7-9]. They are present on most cells of the human body and play crucial roles in mechanosensation, photoreception, intracellular signaling, and fluid movement. Cilia in the embryonic node break left-right symmetry by rotating clockwise to generate leftward fluid flow. Genetic defects in the structure and function of cilia are associated with a range of disorders termed ciliopathies including organ laterality defects, polydactyly (extra digits), and polycystic kidney disease [7-9].

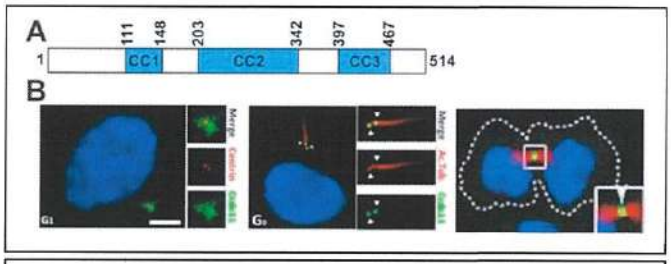

Fig. 1. CCDC 11 structure and localization. (A) CCDC11 consists of 514 aa and contains three coiled-coil (CC) domains. **(B)** CCDC11 localization in RPE1 cells at centrosomes (left), the base of cilia (middle), and the midbody (right). **Source: Modified from Silva et al. 2016 and Ahmed et al. 2018.**

Consistent with CCDC11 being an essential factor for ciliogenesis, it localizes to centrosomes, centriolar satellites, and cilia **(Fig. 1)** [2, 4]. Depletion of CCDC11 from mammalian cultured cells or zebrafish and frog embryos leads to abnormal cilia, resulting in left-right patterning defects [2-5]. Surprisingly, more recently, it was reported that CCDC11 is also important for cell division

[10]. CCDC11 has been shown to localize to the middle region between two dividing daughter cells, called the midbody, in different human cell lines **(Fig. 1)**. Knockdown (KD) of CCDC11 protein in human cultured cells using small interfering RNA (siRNA) blocks cell division, resulting in abnormal cells with two or more nuclei **(Fig. 2)**. Multinucleation is a hallmark of cell division defects due to the failure of cytokinesis, the final phase of mitosis [10]. The Endosomal Sorting Complex Required for Transport III (ESCRT-III) machinery acts in membrane deformation and scission in different biological processes [11-13]. At the end of cytokinesis, ESCRT-III is recruited to the midbody to cleave the intercellular membrane bridge between nascent daughter cells in a process known as abscission [11-13]. Importantly, CCDC11 facilitates the midbody recruitment of Charged Multivesicular Body Protein 2A (CHMP2A), a core subunit of the ESCRT-III complex [10]. At present, the precise molecular roles of CCDC11 in ciliogenesis and cytokinesis are largely unknown.

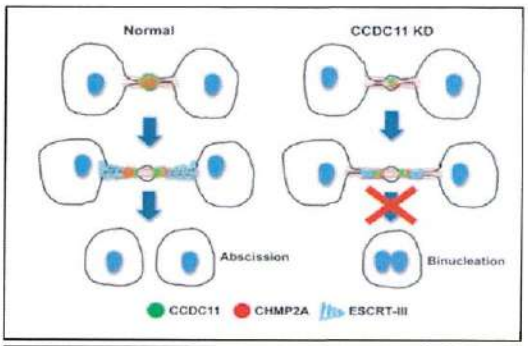

Fig. 2. CCDC11 facilitates the recruitment of CHMP 2A or other ESCRT-III components to the midbody. This may trigger the formation of ESCRT-III filaments, resulting in abscission and production of two new daughter cells. CCDC11-knockdown (KD) cells fail to efficiently recruit CHMP2A, leading to insufficient assembly of the ESCRT-III machinery adjacent to the midbody, failure to complete membrane scission, and the appearance of binucleated cells. **Source: Adapted from Ahmed et al. 2018.**

ESCRT-III has been shown to play an important role for the budding of viral particles from the cell surface [14-17]. Viral buds, small protrusions at the plasma membrane, are initially induced by the assembly of the major HIV-1 structural polyprotein Gag. During final stages of membrane remodeling, the ESCRT machinery is recruited to the sites of viral budding to complete membrane scission and release of mature viral particles from the host cell. ESCRT consists of four distinct subcomplexes (ESCRT-0, -I, -II, and -III) and associated proteins such as Vacuolar Protein

Sorting 4 (Vps4) and the ALG2-Interacting protein X (ALIX) [14, 17, 18]. These ESCRTs are recruited sequentially and transiently to Gag assembly sites. At the final step of viral budding, ESCRT-III, which is composed of CHMP family members, forms spiral filaments that facilitate the constriction of membrane necks to promote viral release. In addition to cytokinetic abscission and viral budding, ESCRTs are implicated in a variety of cellular processes requiring an internal membrane fission event including the formation of MultiVesicular Bodies (MVBs), plasma and nuclear membrane repair, neuronal pruning, and autophagy [19, 20].

With our goal to discover new molecular targets for antiviral therapies against HIV and other harmful viruses, we previously reported that CCDC11 plays a key role in HIV budding [21]. Expression of exogenous CCDC11 robustly increases HIV-1 particle production Human Embryonic Kidney (HEK) 293T cells. Moreover, we successfully generated CCDC11-kockout (KO) HEK293T cells using the CRISPR-Cas9 system and demonstrated that these cells show a marked reduction in production of HIV-1 particles. In our current model for the potential role of CCDC11 in HIV-1 **(Fig. 3)**, in normal cells, CCDC11 is initially recruited to sites of viral budding at the plasma membrane. By analogy to its role in cytokinesis [10], CCDC11 then engages in the recruitment of the ESCRT-III complex, thereby promoting membrane deformation, bud scission and viral release. In contrast, in the absence of CCDC11, the targeting of ESCRT-III is

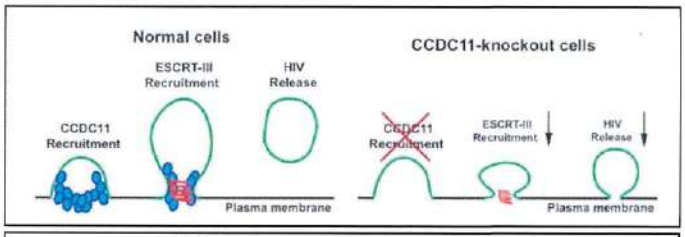

Fig. 3. Model for CCDC11 functions in HIV-1 budding. (Left) In normal cells, HIV-1 Gag structural proteins form clusters at the cell surface to deform plasma membranes. CCDC11 is recruited to the viral budding sites. The ESCRT-III complex such as CHMP2A is then recruited to form spiral filaments to constrict the neck for the budding and release of newly formed viral particles from infected cells. This facilitates HIV release from the cell surface. **(Right)** In CCDC11-knockout (KO) cells, the recruitment of ESCRT-III is reduced, leading to inefficient viral budding. **Source: Student generated model.**

diminished, leading to inefficient viral release. However, the precise molecular functions of CCDC11 in viral budding remain unknown.

In this report, we knocked out CCDC11 in human cervical cancer HeLa cells, which is a widely used model for HIV research, using the CRISPR-Cas9 technology to further extend the role of CCDC11 in the viral budding process. Remarkably, like CCDC11-KO HEK293T cells, CCDC11-KO HeLa cells exhibit a reduced ability to produce HIV-1 particles into cell culture media. In an effort to understand the molecular mechanisms of CCDC11 functions in viral budding, we found that CCDC11 physically interacts with CHMP2A and CHMP4B, both of which are essential for HIV-1 budding. Importantly, we found that CCDC11 localizes to viral budding sites at the plasma membrane. In summary, our findings provide the first evidence that CCDC11 promotes HIV budding through direct recruitment of CHMP2A and CHMP4B to viral budding sites at the plasma membrane.

Materials and Methods

Plasmids and bacterial transformation

Expression plasmids for Flag-tagged human CCDC11 and for HIV-1 pNL4-3-ΔEnv have been described previously [15, 21]. Myc- and Flag-tagged TSG101, HA-tagged ALIX and CHMPs were constructed by subcloning PCR-amplified cDNAs into pCS2+HA mammalian expression vector. The insert sequences were verified by DNA sequencing. All plasmids were transformed into DH5α *E. coli* competent cells (New England Biolabs), and the Qiagen Plasmid Plus Midi Kit was used to purify the plasmid DNAs.

Cell culture and transfection

Human embryonic kidney (HEK) 293T (CRL-3216), HeLa (CCL-2), and U2OS (HTB-96) cells were purchased from American Type Culture Collection (ATCC) and grown in Dulbecco's Modified Eagle Medium (DMEM) and 10% fetal bovine serum (FBS) with 100 U/ml penicillin-streptomycin at 37 °C in a 5% CO_2 incubator. Cells were transfected with Lipofectamine 3000 (Thermo Fisher Scientific) according to the manufacturer's instructions.

Generation of CCDC11-knockout HeLa cells using the CRISPR/Cas9 system

To generate CCDC11-knockout cells using the CRISPR/Cas9 system [22, 23], two short guide RNAs (gRNAs) against the 5' region of the human CCDC11 coding sequence (gRNA-1 and -2) were designed using the CRISPR design tool (http://crispr.mit.edu/): gRNA-1, GCGGTTTGGCACCGTACAGC; gRNA-2, AGCGGTTTGGCACCGTACAG. HEK293T cells were transfected with pSpCas9(BB)-2A-Puro (PX459) V2.0 [22] (Addgene plasmid 62988) containing a human CCDC11 gRNA using Lipofectamine 3000. The empty vector was transfected as a negative control. Transfected cells were selected in the presence of puromycin (2.5 ug/ml). Following 1-2 weeks of culture, multiple single colonies were isolated and further grown for experiments.

gRNAs escort Cas9 nucleases to specific target genomic sites and generate double-strand breaks, which are repaired by error-prone non-homologous end joining (NHEJ), thereby inducing short insertions and deletions (indels). To determine CCDC11-knockout mutations, genomic DNAs were isolated from the cell colonies, and PCR fragments encompassing the gRNA sequence were generated using GoTaq DNA polymerase (Promega) and used for sequencing at the Genomics Core Facility at the Stony Brook University. The primers used to amplify CCDC11

genomic fragments are: 403-bp amplicon, 5'-ATGGTGACCAGACCGACTTC-3' and 5'-GGTGAGCGACCTTATCTTCC-3'.

Western blotting

WT and CCDC11-knockout HeLa cells were harvested and lysed in the radioimmunoprecipitation assay (RIPA) buffer (20 mM Tris-HCl [pH 7.5], 150 mM NaCl, 1 mM EDTA, 1 mM EGTA, 1% Nonidet P-40 [NP-40], 0.5% Sodium deoxycholate, and 0.1% SDS) with protease cocktail inhibitors (Roche) added before use, followed by sonication. The lysates were centrifuged at 13,000 rpm, and supernatant was collected and mixed with 5x SDS sample buffer, followed by denaturing the proteins at 95 °C for 3 minutes. The samples were loaded onto a 10% SDS-polyacrylamide gel electrophoresis (PAGE), and the gel was run for 2 hours at 90 V. Proteins were transferred from the gel onto the nitrocellulose membrane (0.45 μm) (Bio-Rad) with a power supply running at 16 V for 14 hours. The membrane was then washed with Tris-buffered saline with 0.1% Tween 20 (TBST) and blocked in 5% skim milk for 1 hour at room temperature. Rabbit anti-CCDC11 primary antibody (Sigma-Aldrich, HPA040595, 1:500), mouse anti-β-actin antibody (Proteintech, 60008-1-Ig, 1:5,000), mouse anti-Flag M2 antibody (Sigma-Aldrich, F3165, 1:500), or rat anti-HA antibody (Roche, 11867431001, 1:500) was added, followed by incubation for 1 hour. The membrane was washed 3 times for 15 minutes each with TBST. Secondary antibodies conjugated with horseradish peroxidase were added and incubated for 1 hour at room temperature. Antibodies were then removed, and the membrane was washed with TBST 3 times for 15 minutes each. SuperSignal™ West Pico Chemiluminescent Substrate (Thermo Fisher Scientific) was used to detect the proteins of interest on X-ray films.

Immunofluorescence staining

HeLa and U2OS cells were grown on glass coverslips in a 12-well plate for 24-48 hours. The cells were then washed and fixed with cold 50% methanol/50% acetone. The fixed cells were incubated for 1 hour in 300 µl of blocking buffer containing 5% goat serum in diluent solution (2% bovine serum albumin [BSA] and 0.2% Triton X-100 in PBS). The blocking buffer was discarded, and the cells were incubated at 4 °C overnight in 300 µl of the diluent solution containing the following primary antibodies: rabbit anti-CCDC11 (Sigma-Aldrich, HPA040595, 1:300), mouse anti-acetylated α-tubulin (Sigma-Aldrich, T7451, 1:300), rabbit anti-Flag (Sigma-Aldrich, F7425, 1:500), mouse anti-HA (Proteintech, 66066-1-Ig), rabbit anti-GFP (Proteintech, 50430-2-AP, 1:500), and mouse anti-Flag M2 (Sigma-Aldrich, F3165, 1:500). Subsequently, the cells were washed and incubated for 1 hour with appropriate anti-rabbit or anti-mouse IgG secondary antibodies conjugated with DyLight 488 and DyLight 549 (Vector Laboratories). The cells were washed, counterstained with 4′,6-diamidino-2-phenylindole (DAPI), used as a nuclear counterstain, for two minutes at room temperature, washed again, and mounted onto a glass slide using Fluoromount-G (Southern Biotech). The samples were analyzed under a Leica DM6000B epifluorescence microscope, a Leica SP8X confocal microscope, or a Nikon Structured Illumination microscope (SIM). SIM takes 15 images with different illumination patterns, and the raw images are reconstructed into a single super-resolution image. It produces 8-fold higher resolution than conventional confocal microscopy.

Quantification of HIV particle release using p24 ELISA

The HIV-1 Gag protein p24 (MW, 24 kDa) is a structural protein of the HIV-1 capsid. It is initially synthesized as a polyprotein precursor, which is necessary and sufficient for the assembly and production of non-infectious, virus-like particles (VLPs) in the absence of other viral

proteins or packageable viral RNA. Therefore, detectable p24 in cell culture supernatants is strongly correlated to released VLPs. The antigen capture enzyme-linked immunosorbent assay (ELISA) is currently the most common method used to assess viral replication both *in vivo* and *in vitro* for quantitation of the HIV-1 Gag p24 protein.

The day before transfection, HeLa cells were trypsinized and split in triplicate into 6-well plates with 2 ml DMEM culture media. After 18-24 hours, when cells reached 70-90% confluency, either 2ug total DNA were transfected into each well using Lipofectamine 3000 following the manufacturer's protocol. The total amount of plasmid DNA was adjusted using an empty vector if appropriate. An expression plasmid for Renilla luciferase (pRL-TK) (50 ng/well) was cotransfected to normalize transfection efficiency.

After 24-48 hours of transfection, culture media were harvested and clarified by centrifugation to remove cellular debris. We utilized the HIV-1 p24 Capture ELISA kit (ImmunoDX, LLC) to measure the levels of Gag p24 in the culture media by reading the optical densities (O. D.) at a wavelength of 450 nm using a microplate reader. The cells were lysed using 1X passive lysis buffer (Promega) with sonication and used to measure Renilla luciferase activities by the Dual-Luciferase Reporter Assay System (Promega) and a Berthold luminometer (Berthold Technologies). For normalization, the ELISA OD values of Gag p24 were divided by the values of Renilla luciferase activities to account for transfection efficiency. The Y axis in the Figures represents arbitrary units.

Results

Generation of CCDC11-KO HeLa cells

To examine the effect of CCDC11 loss on HIV production in other cell types in addition to HEK293T cells, we chose human cervical cancer HeLa cells that are a widely used model for HIV research. We attempted to generate CCDC11-KO HeLa cells using CRISPR-Cas9 technology as described in Materials and Methods. To validate CCDC11 KO, total cell lysates from a control (V1) and 8 CCDC11-KO candidate clones (g1-1, g1-8, g1-9, g1-11, g1-12, g2-1, g2-12, and g2-14) were prepared and subjected to western blot analysis using anti-CCDC11 antibody **(Fig. 4)**. As expected, there was a single band at the expected size of about 62 kDa for CCDC11 in the control V1 lane. Although g1-9, g1-11, and g1-12 from gRNA-1-transfected cells and g2-1 and g2-14 from gRNA-2-transfected cells retained significant CCDC11 expression, markedly reduced CCDC11 expression was detected in cells transfected with g1-1, g1-8, and g2-12.

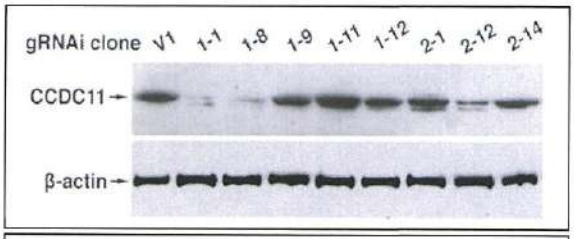

Fig. 4. Western blotting of control and CCDC11 gRNA HeLa cell clones. Cell lysates from the indicated CCDC11 gRNA clones were subjected to western blot analysis using anti-CCDC11 antibody. β-actin served as a loading control. **Source: Student generated data.**

To determine the exact nature of insertion and deletion (indel) mutations in the CCDC11 gene, we purified genomic DNAs from V1, g1-1, g1-8, and g2-12 cell clones and amplified by PCR a 403-bp CCDC11 genomic region encompassing the gRNA sequences. The PCR products were then subcloned into pGEM-T Easy TA vector, followed by restriction digest to verify the presence of an insert. Subsequently, multiple plasmids that carry inserts of the correct size were sequenced **(Fig. 5)**.

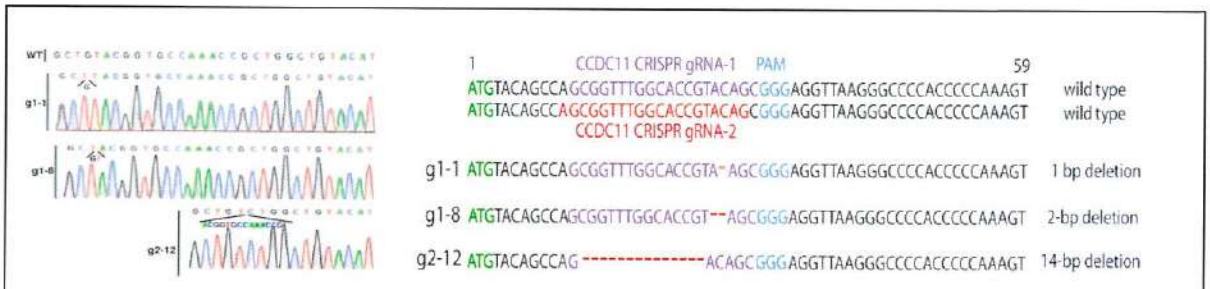

Fig. 5. Genomic DNA sequences of HeLa cell clones g1-1, g1-8, and g2-12 showing deletions. (**Left**) Examples of sequencing chromatograms. (**Right**) Sequencing data were aligned to show deletions. **Source: Student generated data.**

The CCDC11 gene is located on chromosome 18. Consistent with the large decrease in the endogenous protein by western blotting **(Fig. 4)**, g1-1, g1-8, and g2-12 cell lines harbored 1-, 2-, and 14-bp deletions, respectively, causing truncations in the N-terminal region of CCDC11. Despite our efforts in sequencing multiples clones, we were unable to find other mutations. We reasoned that other CCDC11 alleles in these cell lines might contain a deletion or insertion larger than the 403-bp CCDC11 genomic region that we analyzed. Based on these results, we concluded that although g1-1, g1-8, and g2-12 cell lines may not be complete CCDC11-KO, they indeed contain CCDC11 mutations with significantly reduced protein levels. We therefore proceeded to characterization as described below.

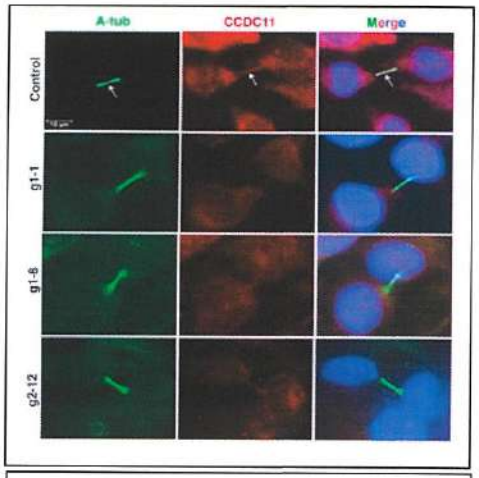

Fig. 6. Reduction of CCDC11 protein at midbody in CCDC11-KO HeLa cells. Control V1 and the CCDC11-KO HeLa cell clones g1-1, g1-8, and g2-12 were immunostained with antibodies for CCDC11 and acetylated α-tubulin (A-tub). Nuclei were visualized by DAPI. A significant decrease in CCDC11 protein at the midbody in the KO cells is evident compared to the control cells as pointed by the arrows. Scale bars, 10 μm. **Source: Student generated data.**

Characterization of CCDC11-KO HeLa cells

To further confirm that g1-1, g1-8, and g2-12 CCDC11-KO HeLa cells show diminished levels of the endogenous protein, we performed immunofluorescence (IF) staining **(Fig. 6)**. In control V1 cells undergoing cytokinesis, clear CCDC11 fluorescence signals were detected at the midbody between the acetylated α-tubulin (A-tub)-positive microtubule bundles, while it was missing or very faint in CCDC11-KO cells. Therefore, these data confirm that these cell lines express little to no CCDC11 protein.

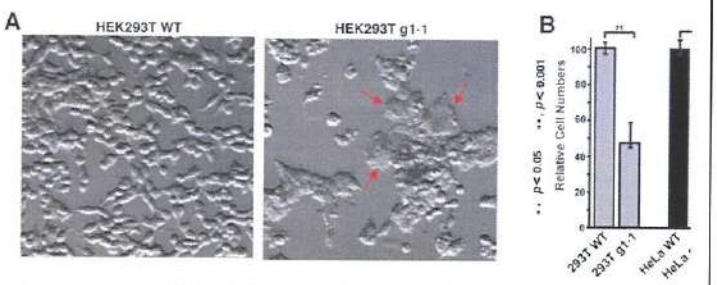

Fig. 7. CCDC11-KO results in slowed growth with multinucleation in HEK293T and HeLa cells. (A) Wild-type (WT) HEK293T and CCDC11-KO g1-1 cells were trypsinized to single cells and counted. Equal numbers of cells of each cell line were seeded in 6-cm plates. After 5 days, cells were imaged under a phase-contrast microscope at a 40x magnification. **(B)** After imaging, the cells were collected and counted. Data are presented as the means ± standard deviations. Student's t-tests were used for statistical analysis, and $p<0.05$ was considered significant. **Source: Student**

CCDC11-KO cells show growth defects

In agreement with its critical role in cytokinesis [10], CCDC11-KO HEK293T and HeLa cells exhibited moderate growth defects with the appearance of multinucleated cells (Fig. 7A) and reduced cell growth in HEK293T and HeLa cells (Fig. 7B) .

CCDC11 is required for efficient HIV particle production in HeLa cells

We examined if loss of CCDC11 influences the production of HIV-1 particles in HeLa cells **(Fig. 8)**. As described previously [21], we utilized ELISA (enzyme-linked immunosorbent assay) for HIV-1 Gag-related capsid protein p24 to evaluate viral particle release. Transfection of an expression plasmid for HIV-1 WT-Gag structural protein into control V1 cells dramatically increased p24 antigen levels in the culture media **(Fig. 8A)**. As a negative control, cells were also transfected with a P7L-Gag expression plasmid harboring a proline-to-leucine substitution in the *gag* gene that impairs Gag binding to Tsg101 [24]. Tsg101, is a component of ESCRT-I that directly binds the P$_7$TAP motif in Gag protein to promote the recruitment of the ESCRT-III

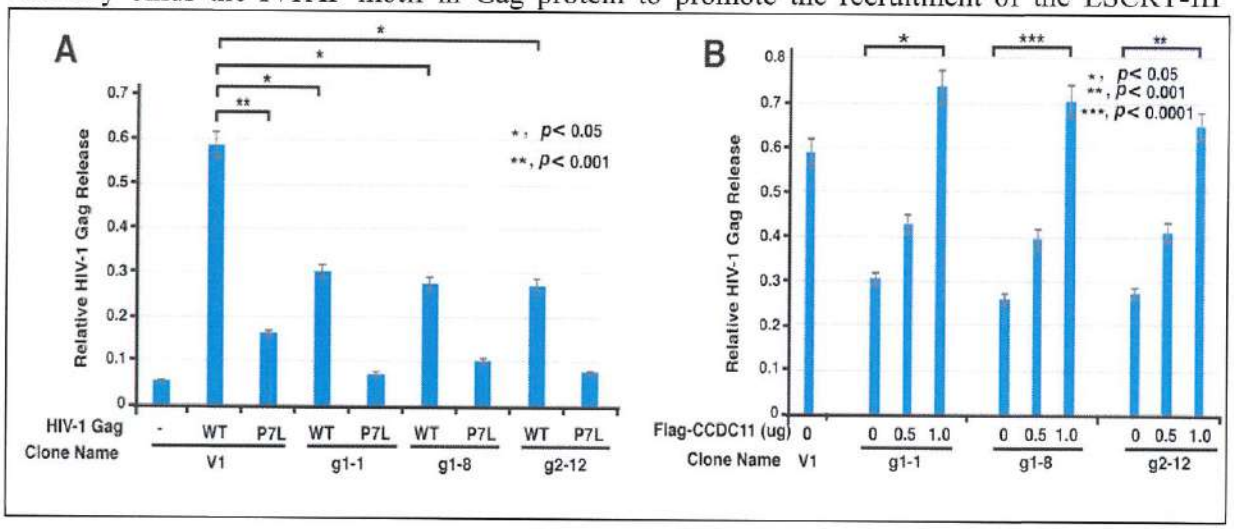

Fig. 8. CCDC11 is required for HIV-1 particle release in HeLa cells. (A) Depletion of CCDC11 reduces HIV-1 particle release. Control (V1) and CCDC11-KO clones (g1-1, g1-8, and g2-12) were transfected in triplicate with a plasmid for HIV-1 WT- or P7L-Gag. **(B)** Re-expression of CCDC11 in the KO cells rescues viral release. CCDC11-KO cells were co-transfected in triplicate with a plasmid for WT-Gag and a plasmid expressing CCDC11 as indicated. An expression plasmid for Renilla luciferase (pRL-TK) was co-transfected to normalize transfection frequency. The tissue culture media were harvested, clarified by centrifugation to remove cellular debris, and used for ELISA. Data are presented as the means ± standard deviations. Student's t-tests were used for statistical analysis , and $p < 0.05$ was considered significant.**Source: Student generated data.**

complex. Expression of P7L-Gag resulted in lower p24 levels in the media. Significantly, transfection of the WT-Gag plasmid into g1-1, g1-4, and g2-12 CCDC11-KO cells yielded low p24 antigen levels. These findings indicate that CCDC11 is required for the efficient production of HIV-1 particles in multiple different cell types.

Next, we performed a rescue experiment by re-introducing CCDC11 back into the CCDC11-KO cells **(Fig. 8B)**. Transient transfection of a CCDC11 expression plasmid into g1-1, g1-4, and g2-12 CCDC11-KO cells robustly increased p24 antigen levels in the culture media in a dose-dependent manner. Taken together, these results confirm and further extend our previous report that CCDC11 plays a crucial role in the production of HIV-1 particles most likely by acting during the viral assembly and/or budding process.

CCDC11 colocalizes with HIV-1 Gag at viral budding sites in HeLa cells

Our data so far demonstrate that CCDC11 is critical for the production of HIV-1 particles. Since CCDC11 is required for the efficient recruitment of CHMP2A to the midbody during cytokinesis [10], we reasoned that CCDC11 is recruited to the sites of viral budding at the plasma membrane, which in turn recruits the ESCRT-III membrane scission machinery to release viral particles. To test this, we co-transfected GFP-tagged Gag and Flag-CCDC11 into HeLa cells and visualized them by IF staining. As shown in **Fig. 9**, Gag localized as punctate foci, representing viral particles produced at plasma membranes. Interestingly, CCDC11 also showed a similar punctate distribution, and some puncta colocalized with Gag (arrows). These results suggest that CCDC11 is recruited to viral budding sites at the plasma membrane.

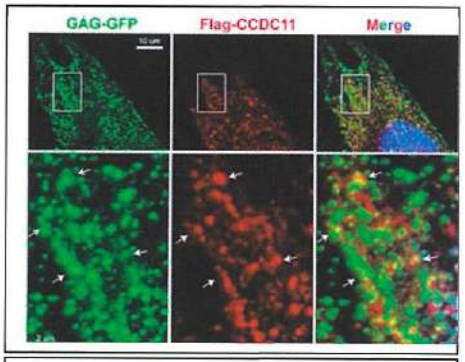

Fig. 9. Visualization of the co-localization of CCDC11 and HIV-1 Gag using confocal microscopy. HeLa cells were co-transfected with Flag-CCDC11 and GFP-tagged Gag and immunostained with anti-Flag antibody for CCDC11 (red) and anti-GFP antibody for Gag (green). Nuclei were visualized by DAPI. Scale bars, 10 μm (top panels); 2 μm (bottom panels). **Source: Student generated data.**

CCDC11 colocalizes with TSG101, CHMP2A, and CHMP4B, but not with ALIX, CHMP6, and CHMP8

The above data suggest that CCDC11 localizes to the right place to initiate the recruitment of the ESCRT-III machinery. To gain insight into the molecular mechanisms, we performed colocalization studies in human osteosarcoma U2OS cells, which is a common cell line used in the field of cell biology. Ectopic expression of CCDC11 alone formed large vesicle-like globular domains of variable sizes **(Fig. 10)**. Interestingly, co-expression of CCDC11 with the major ESCRT-I component TSG101 showed an almost complete overlap. However, we did not observe a colocalization of the auxiliary factor ALIX with CCDC11. Among the ESCRT-III components that we tested, CHMP2A and CHMP4B, but not CHMP6 and CHMP8, colocalized with CCDC11. Especially, the colocalization of CCDC11 and CHMP2A was extensive as revealed by imaging using super-resolution Structured Illumination Microscopy (SIM) **(Fig. 11)**.

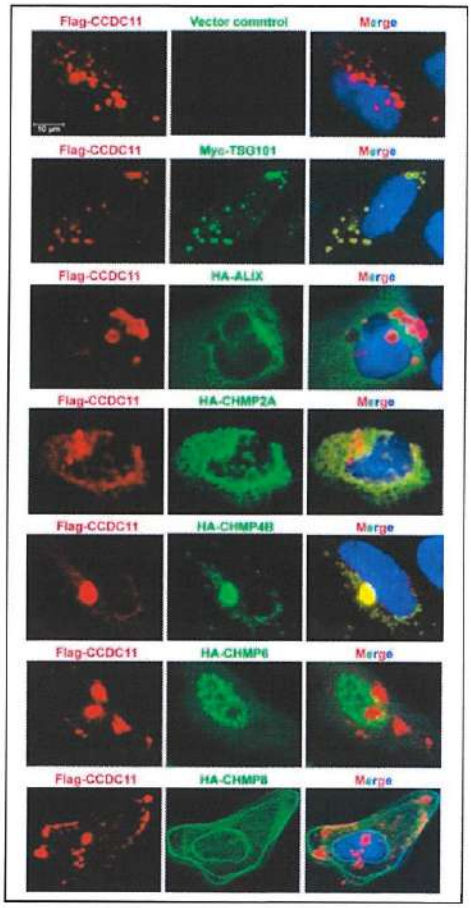

Fig. 10. CCDC11 colocalizes with TSG101, CHMP2A, and CHMP4B, but not with ALIX, CHMP6, and CHMP8. U2OS cells were transfected with Flag-CCDC11 alone or co-transfected with Myc-TSG101, HA-ALIX, or the ESCRT-III components HA-CHMP2A, HA-CHMP4B, HA-CHMP6, or HA-CHMP8, and immunostained with anti-Flag antibody for CCDC11 (red) and anti-Myc or anti-HA antibody for the ESCRT components (green). Nuclei were visualized by DAPI. Scale bar, 10 μm. **Source: Student generated data**.

CCDC11 physically interacts with CHMP2A and CHMP4B

Next, we examined potential physical interactions between CCDC11 and the above ESCRT components using Co-ImmunoPrecipitation assays (Co-IPs) **(Fig. 12)**. As shown in **Fig. 12**,

CCDC11 coimmunoprecipitated CHMP2A and CHMP4B, but not with CHMP6, CHMP8, and ALIX. These data are in line with the above colocalization data and suggest that CCDC11 recruits CHMP2A and CHMP4B to viral budding sites at the plasma membrane and form a complex with TSG101 to facilitate HIV-1 release.

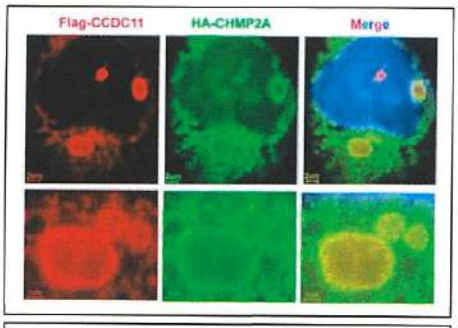

Fig. 11. Visualization of the colocalization of CCDC11 and CHMP2A using the Structured Illumination Microscopy (SIM). U2OS cells were co-transfected with Flag-CCDC11 and HA-CHMP2A and immunostained with anti-Flag antibody for CCDC11 (red) and anti-HA antibody for CHMP2A (green). Nuclei were visualized by DAPI. Scale bars, 2 μm (top panels); 1 μm (bottom panels). **Source: Student generated data.**

Discussion

Here, we report that CCDC11 plays a crucial role in HIV-1 production from HeLa cells in addition to the HEK293T cell model. More excitingly, our research

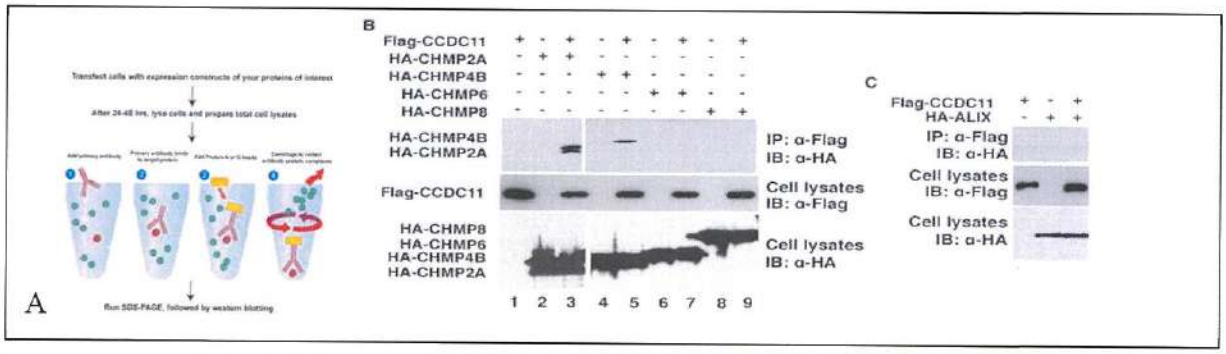

Fig. 12. CCDC11 physically interacts with CHMP2A and CHMP4B but not with CHMP6 and CHMP8. **(A)** Schematic of Co-IP experiments. **Source: Bio-Resource (B)** Flag-CCDC11 was co-transfected with HA-tagged CHMP2A, CHMP4B, CHMP6 or CHMP8 into HEK293T cells, and cell lysates were immunoprecipitated with anti-Flag antibody and detected with anti-HA antibody for the CHMPs. Cell lysates were immunoblotted with anti-Flag antibody for CCDC11, and anti-HA antibody for the CHMPs to confirm stable protein expression. **(C)** Flag-CCDC11 was co-transfected with HA-tagged ALIX into HEK293T cells, and cell lysates were immunoprecipitated with anti-Flag antibody and detected with anti-HA antibody for ALIX. Cell lysates were immunoblotted with anti-Flag antibody for CCDC11 and anti-HA antibody for ALIX to confirm stable protein expression. **Source: Student generated data**

suggests a new molecular model in which TSG101 directly or indirectly recruits CCDC11 to the sites of viral budding at the plasma membrane. CCDC11 then interacts with CHMP2A and

CHMP4B, which are essential components for HIV-1 budding, to assemble active ESCRT-III complexes, leading to HIV-1 release.

Ectopic expression of CHMPs is known to form polymers or filaments in mammalian cultured cells [25]. Colocalization of CCDC11 with CHMP2A and CHMP4B suggest that CCDC11 might be a player in the filaments that contribute to the neck constriction of budding HIV-1 viruses.

TSG101 has been shown to play an important role in HIV-1 budding, but ALIX is dispensable although ALIX binds and recruits CHMP4B [26, 27]. It was speculated that TSG101 somehow plays a role in recruitment of CHMP4B to viral budding sites [27]. Our results, for the first time, suggest that CCDC11 is the missing link between TSG101 and CHMP4B. CHMP4B and CHMP2A bind to each other, and this interaction is required for HIV-1 budding [27]. Thus, it is likely that CCDC11 forms a stable complex with CHMP4B and CHMP2A. Clearly, further experiments are required to gain more insight into the molecular mechanisms of CCDC11 functions in viral budding.

Conclusions

Our research confirms that CCDC11 plays a more general role in HIV budding from different cell types. Mechanistically, CCDC11 is recruited to viral budding sites by TSG101 and then initiates the assembly of the ESCRT-III membrane scission machinery through protein-protein interactions with CHMP2A and CHMP4B.

Future Work

Our results provide fist evidence that CCDC11 interacts with ESCRT components. However, at present, it is not known about the detailed molecular mechanisms of CCDC11 function in HIV-

1 budding. Future projects will focus on: 1) Can we visualize a reduction in HIV-1 release from the surface of CCDC11-knockout cells and/or do HIV-1 budding stall on the surface of CCDC11-knockout cells? 2) In CCDC11-KO cells, is there a reduction in the recruitment of CHMP2A and CHMP4B?; 3) Is CCDC11 recruited to viral budding sites in the absence of TSG101?; 4) Which domain of CCDC11 binds to CHMP2A and CHMP4B?; 5) Do CCDC11-CHMP interactions also important for ciliogenesis and cytokinesis? Through these studies, we hope to learn about new CCDC11 functions and explore unknown areas of viral budding, cytokinesis, and cytokinesis.

References

1. Perles Z, Cinnamon Y, Ta-Shma A, Shaag A, Einbinder T, Rein AJ, et al. A human laterality disorder associated with recessive CCDC11 mutation. J Med Genet. 2012;49(6):386-90. doi: 10.1136/jmedgenet-2011-100457. PubMed PMID: 22577226.

2. Silva E, Betleja E, John E, Spear P, Moresco JJ, Zhang S, et al. Ccdc11 is a novel centriolar satellite protein essential for ciliogenesis and establishment of left-right asymmetry. Mol Biol Cell. 2016;27(1):48-63. doi: 10.1091/mbc.E15-07-0474. PubMed PMID: 26538025; PubMed Central PMCID: PMCPMC4694761.

3. Noel ES, Momenah TS, Al-Dagriri K, Al-Suwaid A, Al-Shahrani S, Jiang H, et al. A Zebrafish Loss-of-Function Model for Human CFAP53 Mutations Reveals Its Specific Role in Laterality Organ Function. Hum Mutat. 2016;37(2):194-200. doi: 10.1002/humu.22928. PubMed PMID: 26531781.

4. Narasimhan V, Hjeij R, Vij S, Loges NT, Wallmeier J, Koerner-Rettberg C, et al. Mutations in CCDC11, which encodes a coiled-coil containing ciliary protein, causes situs inversus due to dysmotility of monocilia in the left-right organizer. Hum Mutat. 2015;36(3):307-18. doi: 10.1002/humu.22738. PubMed PMID: 25504577.

5. Gur M, Cohen EB, Genin O, Fainsod A, Perles Z, Cinnamon Y. Roles of the cilium-associated gene CCDC11 in left-right patterning and in laterality disorders in humans. Int J Dev Biol. 2017;61(3-4-5):267-76. doi: 10.1387/ijdb.160442yc. PubMed PMID: 28621423.

6. Nonaka S, Shiratori H, Saijoh Y, Hamada H. Determination of left-right patterning of the mouse embryo by artificial nodal flow. Nature. 2002;418(6893):96-9. doi: 10.1038/nature00849. PubMed PMID: 12097914.

7. Goetz SC, Anderson KV. The primary cilium: a signalling centre during vertebrate development. Nature reviews Genetics. 2010;11(5):331-44. doi: 10.1038/nrg2774. PubMed PMID: 20395968; PubMed Central PMCID: PMC3121168.

8. Nigg EA, Raff JW. Centrioles, centrosomes, and cilia in health and disease. Cell. 2009;139(4):663-78. doi: 10.1016/j.cell.2009.10.036. PubMed PMID: 19914163.

9. Hildebrandt F, Benzing T, Katsanis N. Ciliopathies. The New England journal of medicine. 2011;364(16):1533-43. doi: 10.1056/NEJMra1010172. PubMed PMID: 21506742; PubMed Central PMCID: PMC3640822.

10. Ahmed A, Lee J, Parker JE, Rizvon A, Nyayapathi V, Li FQ, et al. The cilium- and centrosome-associated protein CCDC11 is required for cytokinesis via midbody recruitment of the ESCRT-III membrane scission complex subunit CHMP2A. J Emerging Investigators. 2018.

11. Mierzwa B, Gerlich DW. Cytokinetic abscission: molecular mechanisms and temporal control. Dev Cell. 2014;31(5):525-38. doi: 10.1016/j.devcel.2014.11.006. PubMed PMID: 25490264.

12. Nahse V, Christ L, Stenmark H, Campsteijn C. The Abscission Checkpoint: Making It to the Final Cut. Trends Cell Biol. 2017;27(1):1-11. doi: 10.1016/j.tcb.2016.10.001. PubMed PMID: 27810282.

13. Olmos Y, Carlton JG. The ESCRT machinery: new roles at new holes. Curr Opin Cell Biol. 2016;38:1-11. doi: 10.1016/j.ceb.2015.12.001. PubMed PMID: 26775243; PubMed Central PMCID: PMCPMC5023845.

14. Hurley JH, Cada AK. Inside job: how the ESCRTs release HIV-1 from infected cells. Biochem Soc Trans. 2018;46(5):1029-36. doi: 10.1042/BST20180019. PubMed PMID: 30154094; PubMed Central PMCID: PMCPMC6277019.

15. Strickland M, Ehrlich LS, Watanabe S, Khan M, Strub MP, Luan CH, et al. Tsg101 chaperone function revealed by HIV-1 assembly inhibitors. Nat Commun. 2017;8(1):1391. Epub 2017/11/11. doi: 10.1038/s41467-017-01426-2. PubMed PMID: 29123089; PubMed Central PMCID: PMCPMC5680296.

16. Usami Y, Popov S, Popova E, Inoue M, Weissenhorn W, H GG. The ESCRT pathway and HIV-1 budding. Biochem Soc Trans. 2009;37(Pt 1):181-4. Epub 2009/01/16. doi: 10.1042/BST0370181. PubMed PMID: 19143627.

17. Martin-Serrano J, Neil SJ. Host factors involved in retroviral budding and release. Nat Rev Microbiol. 2011;9(7):519-31. Epub 2011/06/17. doi: 10.1038/nrmicro2596. PubMed PMID: 21677686.

18. Henne WM, Buchkovich NJ, Emr SD. The ESCRT pathway. Dev Cell. 2011;21(1):77-91. doi: 10.1016/j.devcel.2011.05.015. PubMed PMID: 21763610.

19. Christ L, Raiborg C, Wenzel EM, Campsteijn C, Stenmark H. Cellular Functions and Molecular Mechanisms of the ESCRT Membrane-Scission Machinery. Trends Biochem Sci. 2017;42(1):42-56. doi: 10.1016/j.tibs.2016.08.016. PubMed PMID: 27669649.

20. Alfred V, Vaccari T. When membranes need an ESCRT: endosomal sorting and membrane remodelling in health and disease. Swiss Med Wkly. 2016;146:w14347. doi: 10.4414/smw.2016.14347. PubMed PMID: 27631343.

21. Takemaru L, Pandya P, Lake MW, Carter CA, Li FQ. Investigating the Role of the Novel ESCRT-III Recruitment Factor CCDC11 in HIV Budding: Identifying a Potential Target for Antiviral Therapy. J Emerging Investigators. 2020.

22. Ran FA, Hsu PD, Wright J, Agarwala V, Scott DA, Zhang F. Genome engineering using the CRISPR-Cas9 system. Nat Protoc. 2013;8(11):2281-308. Epub 2013/10/26. doi: 10.1038/nprot.2013.143. PubMed PMID: 24157548; PubMed Central PMCID: PMCPMC3969860.

23. Yan Q, Xu K, Xing J, Zhang T, Wang X, Wei Z, et al. Multiplex CRISPR/Cas9-based genome engineering enhanced by Drosha-mediated sgRNA-shRNA structure. Sci Rep. 2016;6:38970. Epub 2016/12/13. doi: 10.1038/srep38970. PubMed PMID: 27941919; PubMed Central PMCID: PMCPMC5150520.

24. Medina G, Pincetic A, Ehrlich LS, Zhang Y, Tang Y, Leis J, et al. Tsg101 can replace Nedd4 function in ASV Gag release but not membrane targeting. Virology. 2008;377(1):30-8. Epub 2008/06/17. doi: 10.1016/j.virol.2008.04.024. PubMed PMID: 18555885; PubMed Central PMCID: PMCPMC2528022.

25. Cashikar AG, Shim S, Roth R, Maldazys MR, Heuser JE, Hanson PI. Structure of cellular ESCRT-III spirals and their relationship to HIV budding. Elife. 2014;3. Epub 2014/06/01. doi: 10.7554/eLife.02184. PubMed PMID: 24878737; PubMed Central PMCID: PMCPMC4073282.

26. McCullough J, Colf LA, Sundquist WI. Membrane fission reactions of the mammalian ESCRT pathway. Annu Rev Biochem. 2013;82:663-92. doi: 10.1146/annurev-biochem-072909-101058. PubMed PMID: 23527693; PubMed Central PMCID: PMCPMC4047973.

27. Morita E, Sandrin V, McCullough J, Katsuyama A, Baci Hamilton I, Sundquist WI. ESCRT-III protein requirements for HIV-1 budding. Cell Host Microbe. 2011;9(3):235-42. doi: 10.1016/j.chom.2011.02.004. PubMed PMID: 21396898; PubMed Central PMCID: PMCPMC3070458.